Heliyon 6 (2020) e04172

Contents lists available at ScienceDirect

Heliyon

journal homepage: www.cell.com/heliyon

Research article

Analysis of local gyrification index using a novel shape-adaptive kernel and the standard FreeSurfer spherical kernel – evidence from chronic schizophrenia outpatients☆

Olga Płonka [a], Alicja Krześniak [a,b], Przemysław Adamczyk [a,*]

[a] Institute of Psychology, Jagiellonian University, Krakow, Poland
[b] Laboratory of Brain Imaging, Nencki Institute of Experimental Biology, Warsaw, Poland

ARTICLE INFO

Keywords:
Neuroscience
Nervous system
Neuroanatomy
Mental disorder
Clinical psychology
Mental health
Psychological disorders
Adaptive kernel
Cmorph
Local gyrification index
Schizophrenia
Spherical kernel

ABSTRACT

Schizophrenia can be considered a brain disconnectivity condition related to aberrant neurodevelopment that causes alterations in the brain structure, including gyrification of the cortex. Literature findings on cortical folding are incoherent: they report hypogyria in the frontal, superior-parietal and temporal cortices, but also frontal hypergyria. This discrepancy in local gyrification index (LGI) results could be due to the commonly used spherical kernel (Freesurfer), which is a method of analysis that is still not spatially precise enough. In this study we would like to test the spatial accuracy of a novel method based on a shape-adaptive kernel (Cmorph). The analysis of differences in gyrification between chronic schizophrenia outpatients (n = 30) and healthy controls (n = 30) was conducted with two methods: Freesurfer LGI and Cmorph LGI. Widespread differences in the LGI between schizophrenia outpatients and healthy controls were found using both methods. Freesurfer showed hypogyria in the superior temporal gyrus and the right temporal pole; it also showed hypergyria in the rostral-middle-frontal cortex in schizophrenia outpatients. In comparison, Cmorph revealed that hypergyria is equally represented as hypogyria in orbitofrontal and central brain regions. The clusters from Cmorph were smaller and distributed more broadly, covering all lobes of the brain. The presented evidence from disrupted cortical folding in schizophrenia indicates that the shape-adaptive kernel approach has a potential to improve the knowledge on the disrupted cortical folding in schizophrenia; therefore, it could be a valuable tool for further investigation on big sample size.

1. Introduction

The core of psychopathological symptoms in schizophrenia is thought to be an effect of disrupted functional and structural connectivity in the brain that is related to aberrant neurodevelopment, which is believed to start at the same time as the formation of the brain tissues (Friston and Frith, 1995; Friston et al., 2016; Pettersson-Yeo et al., 2011). It is postulated that disconnectivity can have an impact on other neurodevelopmental processes, such as synaptic pruning and myelinogenesis (Cassoli et al., 2015; Rapoport et al., 2012). Moreover, tension-induced growth of white matter is considered able to modulate the folding patterns of the cortical surface (Garcia et al., 2018). In an attempt to better characterize neurodevelopmental underpinnings and identify connectivity alternations in schizophrenia, some recent studies have focused on cortical gyrification (Matsuda and Ohi, 2018), which can be defined as a process of cortical folding in which the initially smooth surface begins to buckle in order to fit into a relatively small space in the skull (Garcia et al., 2018). The most common measure of cortical folding is the gyrification index (GI), which is the ratio of the length of the outer folded surface of the brain to the length of the outer surface excluding sulci (Zilles et al., 1988). Briefly, brains with a higher degree of cortical folding have larger GI values. Initially, this method involved manual GI tracing, which relied on measurements collected by hand from coronal plane slices, often on post-mortem or 2D MRI brain slices (Zilles et al., 1988). Besides the fact that this was expensive and time-consuming, the main criticisms were related to the precision and accuracy of estimation of the architectural complexity of cortical folding because this was captured in only two dimensions (i.e. 2D-related underestimation tendency). Subsequently, the automated GI method was introduced (Moorhead et al., 2006), followed by the local gyrification index (LGI, Schaer et al., 2008).

☆ The study was conducted by the Krakow Schizophrenia Research Group, Krakow, Poland.

* Corresponding author.
E-mail address: przemyslaw.adamczyk@mailplus.pl (P. Adamczyk).

https://doi.org/10.1016/j.heliyon.2020.e04172
Received 18 January 2020; Received in revised form 19 May 2020; Accepted 4 June 2020
2405-8440/© 2020 Published by Elsevier Ltd. This is an open access article under the CC BY-NC-ND license (http://creativecommons.org/licenses/by-nc-nd/4.0/).

The latter, in contrast to a single-point 2D measure, introduces the 3D spherical kernel concept and defines LGI as an area ratio between the outer hull and the pial surface. This method quickly gained popularity as it is more accurate, is accessible from open-source FreeSurfer software (http://surfer.nmr.mgh.harvard.edu/), and is widely used in clinical studies (Matsuda and Ohi, 2018). Importantly, some authors suggest that alterations in cortical folding measured with LGI may be regarded as a biomarker of schizophrenia (Matsuda and Ohi, 2018; White and Hilgetag, 2011). However, consistent conclusions are precluded by the discrepancies between the LGI results in the literature, indicating that abnormalities are more related to increased (hypergyria) or decreased (hypogyria) LGI (Nenadic et al., 2015; Palaniyappan et al., 2011; Sasabayashi et al., 2016, 2019). Previous studies on LGI in schizophrenia have mostly reported global suppression of cortical folding in comparison to healthy controls (White and Hilgetag, 2011). So far, hypogyria has been found mainly in the frontal, superior-parietal and temporal cortices (Cao et al., 2017; Kubera et al., 2018; Yan et al., 2019), as well as in the temporal lobes (Spalthoff et al., 2018), the anterior (Cao et al., 2017) and posterior cingulate cortex (Wheeler and Harper, 2007), the supramarginal gyrus (Cao et al., 2017; Kubera et al., 2018), the insula (Palaniyappan et al., 2013), the visual cortex (V1, V2, V5) (Schultz et al., 2012, 2013), and the multimodal association cortex (Palaniyappan and Liddle, 2012). Importantly, gyrification decreases over the lifespan (a natural consequence of ageing) faster in schizophrenia than in healthy subjects (Cao et al., 2017). Moreover, hypogyria has been detected in people with high-risk (Damme et al., 2019; Nelson et al., 2018) and polygenic risk of schizophrenia (Liu et al., 2016a), thus accentuating the connection between these changes and neurodevelopmental and genetic-risk factors (Matsuda and Ohi, 2018). Lastly, comparative research including other psychiatric diagnoses indicates that LGI changes are more severe than for, e.g., bipolar disorder (Cao et al., 2017; Nenadic et al., 2015) and exist in the broad spectrum of schizophrenic psychoses (Nanda et al., 2014; Sasabayashi et al., 2019).

On the other hand, along with the aforementioned hypogyria findings, some post-mortem (Vogeley et al., 2000), manual tracing or automated GI studies have revealed hypergyrification of the prefrontal cortex in chronic schizophrenia patients (Janssen et al., 2014; Schultz et al., 2010; Vogeley et al., 2000) and in non-affective first-episode psychosis subjects (Zuliani et al., 2018). Furthermore, using surface-based LGI methods, Palaniyappan and Liddle (2012) showed both hypogyrification and hypergyrification in the prefrontal cortex. Moreover, hypergyria in the precuneus and the superior parietal cortex (Kubera et al., 2018) and in the visual cortex (Schultz et al., 2013) have been reported in schizophrenia with the same LGI method.

When summarizing the evidence and the inconsistency of the existing results in the literature, the following questions still seem to be insufficiently resolved: a) is schizophrenia particularly characterized by hypogyria, hypergyria, or both?; b) are the methods used sufficiently spatially sensitive and morphologically exact to detect these cortical folding abnormalities accurately? To tackle the problem of the large amount of spatial (non-linear) data, researchers have incorporated kernel estimation into analyses in a broad range of scientific disciplines, e.g. robotics (Liu et al., 2016b; Sugiyama et al., 2008) and geodesy (Grazzini and Soille, 2009; Yuan et al., 2019). From this perspective, analysis of brain gyrification can be compared and treated by analogy as, for example, an irregular, uneven terrain with cortical gyri as mountains and sulci as valleys. A novel measure of cortical folding and applying kernel estimation was introduced to neuroimaging studies by Lyu et al. (2018) and has the potential to become a useful tool in answering questions related to brain morphology (topography) research. This method comes from the (cortex) shape-adaptive kernel approach, which makes it possible to determine the shape and size of the kernel with regard to local folding and characteristics of the cortex, e.g. sulcal fundi and gyral crowns, in order to better fit in a single sulcus or gyrus without overlapping on neighbouring regions (for detail see: Lyu et al., 2018). This novel method, by better adaptation to real brain morphology, seems in this regard to strongly improve the surface-based spherical kernel method (FreeSurfer LGI, Schaer et al., 2008, 2012). Moreover, the shape-adaptive kernel method (Cmorph LGI, Lyu et al., 2018) makes it possible to capture folding patterns appropriately across the entire cortical surface, whereas the spherical kernel in standard LGI needs to be very big to not sink into, e.g., the Sylvian fissure. As a result, the analysed surface is much more biologically plausible and seems to be more accurate than in previously used methods (e.g. the standard pipeline implemented in FreeSurfer). For example, a kernel area of 316 mm^2 corresponds to the area of a spherical kernel with a radius of 10 mm, while the default in LGI is 25 mm (Lyu et al., 2018).

In the present paper, we aimed to test the spatial accuracy of the novel cortical shape-adaptive kernel (Cmorph, Lyu et al., 2018) and the standard pipeline of the spherical kernel (FreeSurfer, Schaer et al., 2008, 2012) when analysing the between-group differences of chronic schizophrenia outpatients and healthy controls.

2. Material and methods

2.1. Subjects

The study included two groups: schizophrenia outpatients (n = 30) and healthy controls matched in sex, age and education (n = 30). Procedures were designed in accordance with the ethical standards of the World Medical Association Declaration of Helsinki (2013) and approved by the Research Ethics Committee at the Institute of Psychology, Jagiellonian University, Krakow, Poland. All subjects gave informed consent to participate in the experimental procedures: interview, Montreal Cognitive Assessment (MoCA; Nasreddine et al., 2005) and MRI scanning. Additionally, in the clinical group experienced psychiatrists verified the schizophrenia diagnoses and performed the assessment with the Positive and Negative Syndrome Scale (PANSS; Kay et al., 1987; Vandergaag et al., 2006) and the Brief Negative Symptom Scale (BNSS; Kirkpatrick et al., 2011). All clinical subjects were under antipsychotic medication and in a stable psychopathological condition for at least several weeks prior to the assessment. The mean dose of antipsychotics calculated as chlorpromazine equivalents (Atkins et al., 1997; Gardner et al., 2010; Woods, 2003). None of the subjects had a history of head injuries, seizures, substance dependence or any serious current somatic illnesses. All were remunerated after the MRI session. The groups did not differ in terms of sex and age, but they did differ in years of education (CON > SCH), however this difference was not found at the education level ($Chi^2 = 4.592$; $p = 0.204$). A difference in cognitive performance (MoCA) was found, with a lower total score in SCH group revealing the cognitive impairments characteristic for the schizophrenia (Adamczyk et al., 2016). The details are presented in Table 1.

2.2. Image acquisition

Magnetic resonance imaging (MRI) was performed with a 3T scanner (Magnetom Skyra, Siemens) at Malopolska Centre of Biotechnology, Krakow, Poland. Acquisition was performed with a 64-channel head coil. For high-resolution anatomical T1 scans, an optimized magnetization-prepared rapid acquisition gradient echo (MPRAGE) was used with following parameters: TR = 1800 ms, TE = 2.26 ms, TI = 900 ms, FA = 8°, voxel size of 1.0 × 1.0 × 1.0mm, number of sagittal slices = 208, FOV = 256 × 256 mm2, GRAPPA acceleration factor 3, and phase encoding A/P. Whole brain images were covered with axial slices with a 20% gap between slices (distant factor = 0.5 mm), taken in an interleaved, ascending fashion.

2.3. Analysis

Firstly, for the reconstruction of the cortical surfaces and further calculation of the LGI, the standard FreeSurfer v6.0.0 (http://surfer.nmr.mgh.harvard.edu/) pipeline was applied to subjects' T1 scans (i.e. recon-all command with -all -qcache options; Dale et al., 1999; Fischl et al.,

Table 1. Subjects demographics and clinical data. All clinical subjects were taking antipsychotic medication, including conventional (flupentixol, haloperidol, promazine) and/or atypical (amisulpride, clozapine, olanzapine, risperidone, sulpiride, quetiapine; aripiprazole) antipsychotics. Some patients received antidepressants (escitalopram, paroxetine), anxiolytics (hydroxyzine) and/or mood stabilizers (carbamazepine, lithium, valproic acid). The significance level in all statistical analyses equalled alpha = 0.05.

Please check the layout of Table(s) 1	2	Healthy controls (n = 30)	test for between-group differences
Demographic	Mean (SD)	Mean (SD)	
Age	41.88 (8.83) Min. (27) Max (61)	41.80 (8.68) Min (27) Max (61)	t = 0.72; ns
Sex: male/female	14/16	14/16	$Chi^2 = 0.000$; ns
Education (in years)	15.22 (2.95)	16.30 (2.91)	t = 3.03; p < 0.005
Montral Cognitive Assessment (MoCA)	25.10 (3.64)	27.03 (1.96)	t = -4.841; p < 0.01
Clinical			
Schizophrenia diagnosis (ICD-10):	n (%)		
paranoid (F20.0)	27 (91 %)		
undifferentiated (F20.3)	2 (6 %)		
schizoaffective disorder (F25.0)	1 (3 %)		
Type of pharmacotherapy:			
typical anipsychotics	1 (3%)		
atypical antipsychotics	27 (91%)		
typical and atypical antypsychotics mixed	2 (6%)		
anxiolytics	11 (37%)		
antidepressants	4 (14%)		
mood stabilizers	6 (20%)		
Characteristic of the illness:	Mean (SD)		
duration of psychosis (in years)	17.2 (8.57)		
number of relapses	8.83 (7.33)		
number of hospitalizations	8.6 (5.57)		
chlorpromazine equivalent (mg/day)	425.33 (277.74)		
Positive and Negative Syndrome Scale (PANSS)	Mean (SD)		
total	61.23 (16.01)		
positive	11.3 (4.15)		
negative	16.9 (6.4)		
disorganization	9.53 (3.95)		
excitement	6.07 (2.24)		
emotional distress	9.17 (3.17)		
Brief Negative Symptom Scale (BNSS)			
total	22.03 (13.54)		

1999). The pial and white surfaces were checked (using Freeview v2.0.0) for the occurrence of any obvious errors (e.g. tissue fragments deleted) during the reconstruction process. No manual edits were made. One clinical subject was removed from the analysis due to insufficient reconstruction of the brain.

Secondly, the standard LGI (Schaer et al., 2008, 2012) implemented in FreeSurfer (i.e. the recon-all command with -localGI -qcache -measure pial_lgi options) was computed for all subjects. Oval-shaped regions of interest on the outer surface were matched with the corresponding regions of interest on the inner surface (as a result of using a 25mm spherical kernel at each vertex). The ratio of the cortical surface area to outer surface area was calculated and the values were then placed on the corresponding cortical surface vertices, thus creating a global heat map of the LGI.

Thirdly, a similar vertex-wise LGI map was calculated with the Cmorph v1.2 package (Lyu et al., 2018; https://github.com/ilwoolyu/LocalGyrificationIndex), MATLAB R2019a (MathWorks, Inc., Natick, Massachusetts, United States) and GNU parallel software (Tange, 2011; http://www.gnu.org/software/parallel). As the input we used FreeSurfer pial and white surfaces from each subject and hemisphere, converted to triangular 3D vtk format. The Cmorph method adapts the shape of the LGI kernel to elongate it along the sulcus/gyrus and keep it spherical near any plateaus. To obtain this effect, a tensor field from a geodesic distance (travel-time) map is created. The wavefront propagation along the tensor field enables the program to construct the desired shape-adaptive kernels for the LGI computations at each vertex of the input surfaces.

Then, before group comparison statistics, the average brain surface was constructed for all subjects' vertices by mapping them to common surface space corresponding to the surface locations of the individuals (fsaverage command).

Finally, two separate between-group Generalized Linear Model (GLM) analyses of both LGI measures (Cmorph and FreeSurfer) were performed by whole-brain vertex-wise analysis with permutation-based cluster correction for multiple comparisons (mri_glmfit -sim): 1. group with gender as a silent regressor in the group intercept GLM model; 2. group intercept contrast with gender and age as regressor (DODS option in FreeSurfer). Bidirectional contrasts were applied to both LGI methods (i.e. healthy controls > schizophrenia outpatients, healthy controls < schizophrenia outpatients). All contrasts for between group comparison were visualised by FreeView v.2.0 with smoothing 0 mm FWHM, vertex-wise threshold p = 0.01, and cluster-wise (CWP) threshold at p = 0.001. No additional formal statistical comparison between Cmorph and Freesurfer methods was done, except this described by Lyu et al. (2018).

3. Results

Both LGI measures revealed various bilateral differences between schizophrenia and healthy controls (GLM contrast: group x gender x age).

However, essential differences in cluster sizes, localization, and the output of directional contrasts (i.e. Cluster Growing Summary by mri_surfcluster command) should be clearly pointed out. The spherical kernel LGI analysis (FreeSurfer) revealed 3 bilateral temporal region clusters that indicate hypogyria in schizophrenia and 5 clusters in frontal regions related to hypergyria; total size of hypogyria 1259 mm2; hypergyria 219 mm2. At the same time, the cortex shape-adaptive kernel method (Cmorph) revealed widespread bidirectional differences, i.e. 23 hypogyria clusters (13 left hemisphere/10 right hemisphere) in 18 fronto-temporo-parietal brain regions in both hemispheres, and 25 hypergyria clusters (14 left hemisphere/11 right hemisphere) in 20 fronto-temporo-parieto-occipital brain regions in schizophrenia; total size of hypogyria 994 mm2; hypergyria 1184 mm2. It is noteworthy that the adaptive kernel approach revealed smaller and more precise localized clusters within bidirectional contrasts as compared to the standard FreeSurfer output. Detailed statistics and labelling of cluster annotations are presented in Table 2. Visualization of schizophrenia-related hypogyria (red) and hypergyria (blue) clusters from both assessed LGI methods for group x gender x age GLM model are presented in Figure 1.

4. Discussion

To the best of our knowledge, this is the first study that has attempted to use the cortex shape-adaptive kernel approach in estimating cortical folding differences in schizophrenia. The results obtained from both methods (Cmorph and FreeSurfer) indicate widespread differences in LGI between schizophrenia outpatients and healthy controls. Both methods revealed consistent hypogyria findings in bilateral temporal and frontal hypergyria regions. Additionally, the clusters from the shape-adaptive kernel method are smaller and more spread out across the brain and create more diffuse and complex patterns of bidirectional changes on cortical folding in schizophrenia, i.e. fronto-temporo-parieto-occipital hypogyria and hypergyria. Overall, the presented results indicate that Cmorph LGI may be successfully used for LGI measurement in schizophrenia and other clinical populations.

4.1. Spherical kernel LGI

Firstly, the presented results from the spherical kernel LGI indicated hypogyrification only in the temporal regions (i.e. superior temporal gyrus) of both hemispheres and in the right temporal pole in schizophrenia outpatients. Similar structures were reported previously in people with a high clinical risk of schizophrenia (Damme et al., 2019), and in people with resistant auditory hallucinations (Cachia et al., 2008). Moreover, a big cluster of hypogyria but only in the right superior temporal gyrus in adolescents with schizophrenia was also identified (Palaniyappan et al., 2013). Interestingly, although we found bidirectional changes, the above findings are in line with our results when considering the lateralization shift in the size of the differences, i.e. a big cluster in the right hemisphere (ca. 1200 mm2) vs a small one in the left hemisphere (ca. 40mm2).

Secondly, standard LGI revealed that hypergyria regions in schizophrenia were presented mainly in the rostral-middle-frontal cortex in both hemispheres. This is in line with some previous studies on the prefrontal regions on interest (Nenadic et al., 2015; Sasabayashi et al., 2019; Zuliani et al., 2018) and on whole-brain analysis (Takayanagi et al., 2019). However, another report indicates that observed changes could be related to the greater number of intermediate orbital sulci in some patients (Bartholomeusz et al., 2013). Moreover, an increase in cortical folding has also been detected in the superior-frontal and anterior cingulate regions in the left hemisphere (Sasabayashi et al., 2016; Takayanagi et al., 2019). This is in contrast to previous findings which reported hypogyria in these two structures, i.e. the superior-frontal and anterior cingulate regions (Kubera et al., 2018; Nanda et al., 2014). Finally, other contradictory literature findings showed either only hypogyria in clinical high-risk subjects (Damme et al., 2019) and schizophrenia patients (Cao et al., 2017; Yan et al., 2019) or, in contrast, unidirectional hypergyria in schizophrenia patients (Sasabayashi et al., 2019; Takayanagi et al., 2019). All these mutually exclusive results are at the source of this far-reaching dispute over whether abnormal neurodevelopment of the cortex in schizophrenia results in hypogyria, hypergyria, or both.

4.2. Hypogyria vs. hypergyria in schizophrenia

Hypergyria may be related to altered brain neurodevelopment and maturation. It is believed that axonal tension is not sufficient to induce cortical folding, but tension-induced growth of white matter could modulate the folding of the cortex (Garcia et al., 2018). This is in line with studies on white matter in schizophrenia that show widespread disconnectivity in patients (Wheeler and Voineskos, 2014). However, it only explains the source of the differences in cortical gyrification, but not its diversity. Other neurodevelopmental process could have an impact on folding, for example, cell migration. Altered neurodevelopment has an influence on cortical thickness and some findings indicate thinning of the prefrontal cortex in schizophrenia (Nesvåg et al., 2008), which also shows hypergyrification in high genetic risk subjects (Dauvermann et al., 2012). Additionally, as suggested by some authors (Palaniyappan et al., 2013), regions which are involved in deficits in schizophrenia patients, such as the multimodal association cortex, could have altered gyrification (e.g. the superior temporal gyrus, as shown in our study).

'Yet, our results may shift the balance in the discussion towards the existence of both hypogyria and hypergyria in schizophrenia patients, both of which can be detected by the spherical-kernel method but are much more clearly seen with the cortex shape-adaptive kernel approach.

4.3. Cmorph – shape-adaptive kernel LGI

Cmorph methods revealed that hypergyria is equally represented in the schizophrenic brain as hypogyria, which is easily visible in a wide range of fronto-temporo-parieto-occipital brain regions. This may be related to two main factors which stand out when these two methods are compared in terms of their spatial accuracy in identification of regions with altered brain gyrification: cluster size and biological mapping accuracy. In fact, standard LGI shows big clusters covering a few gyri, for example in the right superior-temporal cortex (ca. 1200mm2) (see Figure 1), while clusters from Cmorph LGI are smaller, e.g. three clusters identified in the right superior-temporal region (ca. 105mm2). Moreover, the clusters from Cmorph seem to be more morphologically accurate and can fit into a single gyri/sulci and are thus distributed more broadly across the brain. Results from the shape-adaptive kernel LGI coincide with the spherical kernel LGI, but due to its more relevant measurements (smaller kernel size) Cmorph LGI is able to reveal small differences in regions which would blend into one cluster in standard FreeSurfer LGI. As a result, differences can be detected that are coherent with other studies (Nesvåg et al., 2014; Schmitt et al., 2015; Schultz et al., 2010; Yan et al., 2019) despite the relatively small sample-size examined in our study. For example, the presented findings on hypogyria in the precentral gyrus and the middle frontal regions are complementary with previous studies (Schmitt et al., 2015; Yan et al., 2019) and findings on altered LGI in the right precuneus (Nesvåg et al., 2014) or supramarginal gyrus (Palaniyappan and Liddle, 2012). Finally, the reported hypergyria in the lateral orbitofrontal cortices, rostral middle frontal gyri, and occipital area regions are similar to those pointed out in a study on first-episode schizophrenia patients (Sasabayashi et al., 2016).

4.4. Limitations and future directions

In summary, this is the first Cmorph LGI study on schizophrenia, but some limitations precludes explicit conclusions concerning the unique patterns of cortex folding in schizophrenia. First of all, replication on a bigger sample size is needed and this work should be considered as an

Table 2. Comparison of the between group differences in the LGI obtained with FreeSurfer spherical kernel method and Cmorph shape-adaptive kernel method. Statistical analysis from mri_glmfit –sim utilized a whole-brain vertex-wise analysis with permutation-based cluster correction for multiple comparisons, controlled for age and gender, with smoothing 0 mm FWHM, vertex wise threshold p = 0.01 and cluster wise (CWP) threshold at p = 0.001. Differences are presented as: maximum value of the cluster (Max), maximum value of the vertex (Vtx max), size in mm2 with the MNI coordinates per cluster. Results are reported from both, unidirectional (positive) and bidirectional (absolute) contrasts (healthy controls > schizophrenia outpatients, healthy controls < schizophrenia outpatients).

Spherical kernel LGI								Cortical shape-adaptive kernel LGI							
Cluster Annotation	Max	VtxMax	Size (mm2) positive contrast	Size (mm2) absolute contrast	MNI			Cluster Annotation	Max	VtxMax	Size (mm2) positive contrast	Size (mm2) absolute contrast	MNI		
					X	Y	Z						X	Y	Z
Healthy controls > schizophrenia outpatients															
Left hemisphere															
								lateralorbitofrontal	1.964	20593	17.11	-	-27.9	29.4	1
								medialorbitofrontal	3.092	11982	9.34	17.68	-8.8	10.6	-15.5
								rostralmiddlefrontal	2.506	145943	18.17	37.24	-21.9	53.1	7.4
									2.133	886	16.58	-	-28.9	48.1	2.4
								superiorfrontal	3.975	131494	54.47	68.16	-15	61.3	5.7
								precentral	2.822	34484	101.07	142.02	-42	-6.7	44.1
superiortemporal	2.25	57705	38.92	15.44	-55.9	1.2	-11.9	superiortemporal	2.584	96464	12.62	33.24	-63.6	-20.2	-0.7
									3.769	161219	77.5	122.41	-53.6	5.9	-12.4
									2.38	43353	17.14	-	-60.5	-16.2	2.2
								inferiortemporal	4.374	62831	128.86	161.94	-55.5	-51	-13.1
								fusiform	2.138	57856	9.22	29.93	-28.5	-79.6	-8.9
								precuneus	2.46	162404	42.6	138.78	-26.5	-64.5	6
								superiorparietal	2.32	135824	15.79	-	-10.6	-91.4	27.1
Right Hemisphere															
								caudalmiddlefrontal	3.246	140460	92.28	134.2	38.2	22.2	39.1
								superiorfrontal	2.448	123167	23.76	-	19.2	47.6	32.1
								precentral	2.993	145515	96.84	144.37	39.9	-4.9	44
								paracentral	2.225	66777	17.91	-	14.9	-26	45.2
								postcentral	2.058	59788	10.01	-	23.3	-31	70.4
superiortemporal	4.11	18701	1203.83	741.88	46.5	4	-21.9	superiortemporal	3.155	70390	66.24	97.71	60.2	-1.4	-5.8
									2.735	94495	24.81	58.7	44.9	15.3	-25.1
									2.365	18701	14.31	38.1	46.5	4	-21.9
								inferiortemporal	1.982	5662	16.86	-	53.9	-59.5	-7.6
temporalpole	1.96	143259	15.81	-	39.3	14.6	-31.3								
								lingual	2.331	35907	22.33	-	22.1	-54.2	-7.3
Healthy controls < schizophrenia outpatients															
Left hemisphere															
								medialorbitofrontal	2.319	10739	11.03	-	-5.2	47.8	-22.3
								lateralorbitofrontal	2.57	17304	32.35	81.4	-25.7	23.2	-17.6
									2.076	51061	20.45	-	-13.9	32	-19.5
								parsorbitalis	2.372	73167	11.16	-	-34.6	40.7	-10.2
caudalmiddlefrontal	2.32	47079	66.28	11.04	-27.3	21.3	36	rostralmiddlefrontal	2.425	106449	15.34	27.31	-37.5	50.9	1
superiorfrontal	2.34	67353	50.05	14.85	-20.1	25.6	46.1	superiorfrontal	3.301	47297	127.43	176	-22.1	17.8	41.8
rostralanteriorcingulate	2.47	33175	29.44	9	-7	41.1	2.8	rostralanteriorcingulate	2.728	83315	56.04	125.4	-10.5	37.6	13.1
								bank of superior temporal sulcus	2.097	86620	50.02	-	-50.1	-40.2	-5
								fusiform	2.355	11016	11.32	-	-34	-44	-20.6
								precentral	5.326	63825	126.53	160.78	-54.5	-1.8	37
								inferiorparietal	2.416	8339	15.74	34.45	-51.2	-58.4	27.8
									3.312	111719	201.41	291	-42.2	-52.3	19.2
								lingual	2.501	53460	43.82	92.27	-15.6	-79.6	-11.8
								precuneus	2.185	101451	23.4	-	-14.7	-51.3	33.2
Right Hemisphere															
								lateralorbitofrontal	2.575	134238	27.99	105.38	31.6	30.8	-11.3
rostralmiddlefrontal	2.40	71009	63.04	16.92	37.9	42.6	10.3	rostralmiddlefrontal	4.273	145879	66.81	85.64	37.5	52.4	-4.9
	2.03	97995	10.22	-	42.7	37.9	23.9		2.261	65649	35.28	-	23.5	51.6	20.6

(*continued on next page*)

Table 2 (*continued*)

Spherical kernel LGI								Cortical shape-adaptive kernel LGI							
Cluster Annotation	Max	VtxMax	Size (mm2) positive contrast	Size (mm2) absolute contrast	MNI			Cluster Annotation	Max	VtxMax	Size (mm2) positive contrast	Size (mm2) absolute contrast	MNI		
					X	Y	Z						X	Y	Z
								caudalmiddlefrontal	2.099	124279	21.4	-	37.8	1.9	31.9
									2.025	14059	18.18	-	24.8	5.3	46.8
								middletemporal	2.074	1799	21.76	-	59.6	-21.9	-19.9
								precentral	2.464	82953	12.34	-	57.9	0.6	32.6
									2.416	145233	23.38	56.45	36.1	-20.1	52.8
								fusiform	4.003	114437	70.91	100.14	39.1	-42	-21.2
								supramarginal	3.712	101436	128.01	164.52	48.2	-39.4	40.5
								lateraloccipital	2.26	18885	12.29	26.84	39.2	-86.5	-3.2

inspiration for succeeding studies on the LGI abnormalities in schizophrenia. Nevertheless, besides the greater number of altered hypo- and hypergyria brain regions revealed by new LGI method (Cmorph) than standard FreeSurfer code, due to the limited sample size from our project and no formal statistical comparison of pipelines, we were unable to clearly state which method is more accurate at illustrating the actual cortical folding abnormalities in schizophrenia. In particular, the problem of normalization of individual brain size and chosen kernel size with the average of total cortical surface area over population is widely discussed and the code is still under development. Although, presented preliminary results may serve as valuable pioneering outcome as they point out the problems arising in the field of brain morphometry analyses and indicate the future direction of their development. More specifically, considering the debate over whether changes in LGI might become a biomarker of schizophrenia (Matsuda and Ohi, 2018; Sasabayashi et al., 2019; Veronese et al., 2013), precision in the mapping of brain regions should be a special concern (Bartholomeusz et al., 2013; Ronan et al., 2012). Aberrant LGI is a widely suggested potential biomarker for people with a genetic risk (Schmitt et al., 2015) or clinical high risk of developing schizophrenia (Damme et al., 2019; Dauvermann et al., 2012; Stanfield et al., 2008), or in those who already have schizophrenia (Veronese et al., 2013) and may differentiate subjects' gyrification changes from other psychiatric conditions (Cao et al., 2017; McIntosh et al., 2009). Thus, the application of shape-adaptive kernel Cmorph LGI in big data studies, like the ENIGMA consortium (https://enigma.ini.usc.edu), the Human Connectome Project (http://www.humanconnectomeproject.org/), or the SchizConnect project database (http://schizconnect.org/), could bring consistent results and allow the complex patterns of cortical folding in schizophrenia to be revealed. Furthermore, the shape-adaptive kernel approach could be useful in examining the relation between gyrification and psychopathology in schizophrenia, which has only been examined by a few studies so far that focused on the deficit and negative symptoms (Mihailov et al., 2017; Storvestre et al., 2019; Takayanagi et al., 2019). Finally, Cmorph seems to be a method which can be widely applied in morphometric studies concerning not only schizophrenia but also other clinical conditions related to altered brain structure.

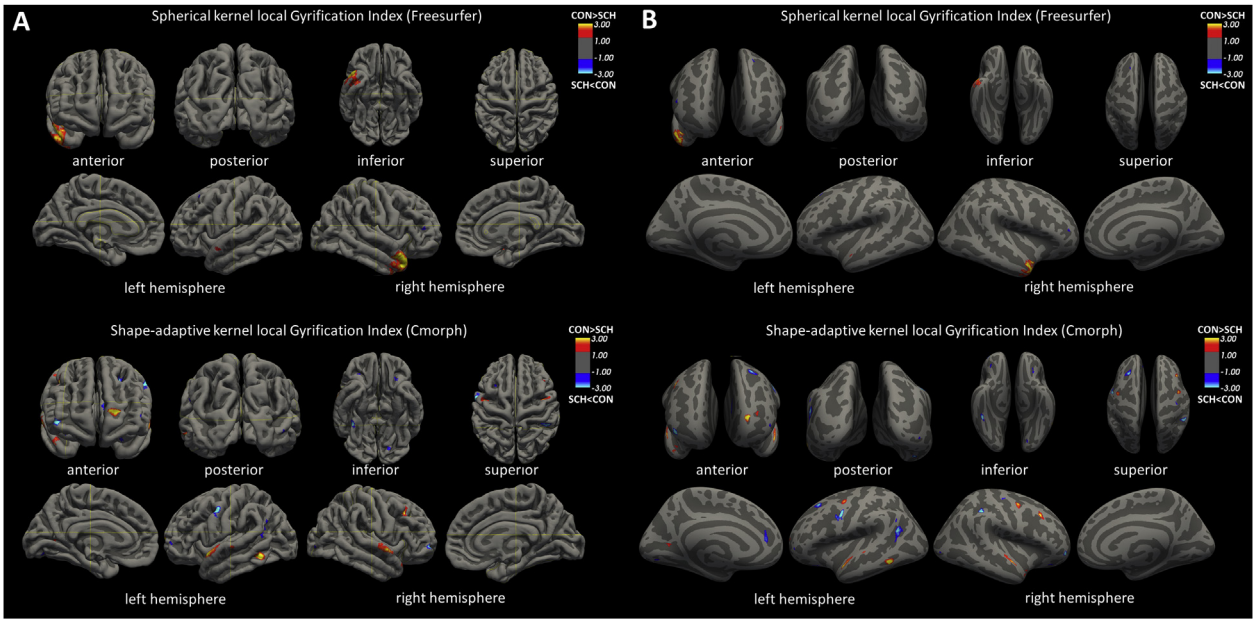

Figure 1. Comparison of between-group differences of the FreeSurfer gyrification index (top panels) and cortex-shape-adaptive kernel Cmorph method (bottom panels) depicted as non-inflated (A panel, on left) or inflated (B panel, on right) pial surfaces. Statistical analysis from mri_glmfit utilized a whole-brain vertex-wise shape analysis with smoothing 0 mm FWHM, vertex-wise threshold $p = 0.01$, and cluster-wise threshold $p = 0.001$. Images of cluster localizations (anterior, posterior, inferior, superior, sagittal lateral/middle plane) were obtained with FreeSurfer (http://surfer.nmr.mgh.harvard.edu/) and visualized with FreeView v.2.0. The colour scale (red: healthy controls > schizophrenia outpatients; blue: healthy controls < schizophrenia outpatients) is set the same for both methods. Coloured areas show the vertex-wise p-values of the difference between patients and controls as $\log_{10}(p)$, so that dark colour (value = 1.3) means $p = 0.05$. The vertex-wise results are masked by the positions of significant clusters.

5. Conclusions

In conclusion, the presented evidence from disrupted cortical folding in schizophrenia outpatients indicates that the cortex shape-adaptive kernel (Cmorph LGI) approach may be a valuable tool for further investigation, especially if a big sample size is involved, as well as in other clinical populations. Finally, presented preliminary results from novel LGI method (Cmorph) suggest that potential mechanism of altered cortical folding in schizophrenia is not related only to the hypogyria, but rather with such changes in brain neurodevelopment, maturation and ageing with final settlement of alternate brain regions morphology (hypo- and hypergyria) and its abnormal connectivity. However, the future investigation should be provided to resolve this question and to better determine biological origins of schizophrenic psychoses.

Declarations

Author contribution statement

Olga Płonka: Performed the experiments; Wrote the paper.

Alicja Krześniak: Analyzed and interpreted the data; Contributed reagents, materials, analysis tools or data.

Przemysław Adamczyk: Conceived and designed the experiments; Performed the experiments; Analyzed and interpreted the data.

Funding statement

This work was supported by the National Science Centre, Poland, grant no 2016/23/B/HS6/00286.

Competing interest statement

The authors declare no conflict of interest.

Additional information

No additional information is available for this paper.

Acknowledgements

We are thankful to all participants in this study, to Dr Piotr Błądziński, Dr Aneta Kalisz and prof. Andrzej Cechnicki for conducting psychiatric assessments and for help in carrying out this work and to Mike Timberlake for proofreading the manuscript.

References

Adamczyk, P., Daren, A., Sułecka, A., Błądziński, P., Cichocki, Ł., Kalisz, A., Gawęda, Ł., Cechnicki, A., 2016. Do better communication skills promote sheltered employment in schizophrenia? Schizophr. Res. 176, 331–339.

Atkins, M., Burgess, A., Bottomley, C., Riccio, M., 1997. Chlorpromazine equivalents: a consensus of opinion for both clinical and research applications. Psychiatr. Bull. 21, 224–226.

Bartholomeusz, C.F., Whittle, S.L., Montague, A., Ansell, B., McGorry, P.D., Velakoulis, D., Pantelis, C., Wood, S.J., 2013. Sulcogyral patterns and morphological abnormalities of the orbitofrontal cortex in psychosis. Prog. Neuro Psychopharmacol. Biol. Psychiatr. 44, 168–177.

Cachia, A., Paillère-Martinot, M.-L., Galinowski, A., Januel, D., de Beaurepaire, R., Bellivier, F., Artiges, E., Andoh, J., Bartrés-Faz, D., Duchesnay, E., Rivière, D., Plaze, M., Mangin, J.-F., Martinot, J.-L., 2008. Cortical folding abnormalities in schizophrenia patients with resistant auditory hallucinations. Neuroimage 39 (3), 927–935.

Cao, B., Mwangi, B., Passos, I.C., Wu, M.-J., Keser, Z., Zunta-Soares, G.B., Xu, D., Hasan, K.M., Soares, J.C., 2017. Lifespan gyrification trajectories of human brain in healthy individuals and patients with major psychiatric disorders. Sci. Rep. 7 (1), 511.

Cassoli, J.S., Guest, P.C., Malchow, B., Schmitt, A., Falkai, P., Martins-de-Souza, D., 2015. Disturbed macro-connectivity in schizophrenia linked to oligodendrocyte dysfunction: from structural findings to molecules. NPJ Schizophrenia 1 (1), 15034.

Dale, A.M., Fischl, B., Sereno, M.I., 1999. Cortical surface-based analysis. I. Segmentation and surface reconstruction. Neuroimage 9 (2), 179–194.

Damme, K.S.F., Gupta, T., Nusslock, R., Bernard, J.A., Orr, J.M., Mittal, V.A., 2019. Cortical morphometry in the psychosis risk period: a comprehensive perspective of surface features. Biol. Psychiatr.: Cogn. Neurosci. Neuroimg. 4 (5), 434–443.

Dauvermann, M.R., Mukherjee, P., Moorhead, W.T., Stanfield, A.C., Fusar-Poli, P., Lawrie, S.M., Whalley, H.C., 2012. Relationship between gyrification and functional connectivity of the prefrontal cortex in subjects at high genetic risk of schizophrenia. Curr. Pharmaceut. Des. 18 (4), 434–442.

Fischl, B., Sereno, M.I., Dale, A.M., 1999. Cortical surface-based analysis. II: inflation, flattening, and a surface-based coordinate system. Neuroimage 9 (2), 195–207.

Friston, K.J., Frith, C.D., 1995. Schizophrenia: a disconnection syndrome? Clin. Neurosci. N. Y. N 3, 89–97.

Friston, K., Brown, H.R., Siemerkus, J., Stephan, K.E., 2016. The dysconnection hypothesis. Schizophr. Res. 176, 83–94.

Garcia, K.E., Kroenke, C.D., Bayly, P.V., 2018. Mechanics of cortical folding: stress, growth and stability. Phil. Trans. Biol. Sci. 373 (1759), 20170321.

Gardner, D.M., Murphy, A.L., O'Donnell, H., Centorrino, F., Baldessarini, R.J., 2010. International consensus study of antipsychotic dosing. Am. J. Psychiatr. 167, 686–693.

Grazzini, J., Soille, P., 2009. Edge-preserving smoothing using a similarity measure in adaptive geodesic neighbourhoods. Pattern Recogn. 42 (10), 2306–2316.

Janssen, J., Alemán-Gómez, Y., Schnack, H., Balaban, E., Pina-Camacho, L., Alfaro-Almagro, F., Castro-Fornieles, J., Otero, S., Baeza, I., Moreno, D., Bargalló, N., Parellada, M., Arango, C., Desco, M., 2014. Cortical morphology of adolescents with bipolar disorder and with schizophrenia. Schizophr. Res. 158 (1–3), 91–99.

Kay, S.R., Fiszbein, A., Opler, L.A., 1987. The positive and negative syndrome scale (PANSS) for schizophrenia. Schizophr. Bull. 13 (2), 261–276.

Kirkpatrick, B., Strauss, G.P., Nguyen, L., Fischer, B.A., Daniel, D.G., Cienfuegos, A., Marder, S.R., 2011. The brief negative symptom scale: psychometric properties. Schizophr. Bull. 37, 300–305.

Kubera, K.M., Thomann, P.A., Hirjak, D., Barth, A., Sambataro, F., Vasic, N., Wolf, N.D., Frasch, K., Wolf, R.C., 2018. Cortical folding abnormalities in patients with schizophrenia who have persistent auditory verbal hallucinations. Eur. Neuropsychopharmacol 28 (2), 297–306.

Liu, B., Zhang, X., Cui, Y., Qin, W., Tao, Y., Li, J., Yu, C., Jiang, T., 2016a. Polygenic risk for schizophrenia influences cortical gyrification in 2 independent general populations. Schizophr. Bull. sbw051.

Liu, C., Wang, Y., Gao, S., 2016b. Adaptive shape kernel-based mean shift tracker in robot vision system. Comput. Intell. Neurosci. 2016, 1–8.

Lyu, I., Kim, S.H., Girault, J.B., Gilmore, J.H., Styner, M.A., 2018. A cortical shape-adaptive approach to local gyrification index. Med. Image Anal. 48, 244–258.

Matsuda, Y., Ohi, K., 2018. Cortical gyrification in schizophrenia: current perspectives. Neuropsychiatric Dis. Treat. 14, 1861–1869.

McIntosh, A.M., Moorhead, T.W.J., McKirdy, J., Hall, J., Sussmann, J.E.D., Stanfield, A.C., Harris, J.M., Johnstone, E.C., Lawrie, S.M., 2009. Prefrontal gyral folding and its cognitive correlates in bipolar disorder and schizophrenia. Acta Psychiatr. Scand. 119 (3), 192–198.

Mihailov, A., Padula, M.C., Scariati, E., Schaer, M., Schneider, M., Eliez, S., 2017. Morphological brain changes associated with negative symptoms in patients with 22q11.2 Deletion Syndrome. Schizophr. Res. 188, 52–58.

Moorhead, T.W.J., Harris, J.M., Stanfield, A.C., Job, D.E., Best, J.J.K., Johnstone, E.C., Lawrie, S.M., 2006. Automated computation of the Gyrification Index in prefrontal lobes: methods and comparison with manual implementation. Neuroimage 31 (4), 1560–1566.

Nanda, P., Tandon, N., Mathew, I.T., Giakoumatos, C.I., Abhishekh, H.A., Clementz, B.A., Pearlson, G.D., Sweeney, J., Tamminga, C.A., Keshavan, M.S., 2014. Local gyrification index in probands with psychotic disorders and their first-degree relatives. Biol. Psychiatr. 76 (6), 447–455.

Nasreddine, Z.S., Phillips, N.A., Bédirian, V., Charbonneau, S., Whitehead, V., Collin, I., Cummings, J.L., Chertkow, H., 2005. The montreal cognitive assessment, MoCA: a brief screening tool for mild cognitive impairment. J. Am. Geriatr. Soc. 53, 695–699.

Nelson, E.A., White, D.M., Kraguljac, N.V., Lahti, A.C., 2018. Gyrification connectomes in unmedicated patients with schizophrenia and following a short course of antipsychotic drug treatment. Front. Psychiatr. 9, 699.

Nenadic, I., Maitra, R., Dietzek, M., Langbein, K., Smesny, S., Sauer, H., Gaser, C., 2015. Prefrontal gyrification in psychotic bipolar I disorder vs. Schizophrenia. J. Affect. Disord. 185, 104–107.

Nesvåg, R., Lawyer, G., Varnäs, K., Fjell, A.M., Walhovd, K.B., Frigessi, A., Jönsson, E.G., Agartz, I., 2008. Regional thinning of the cerebral cortex in schizophrenia: effects of diagnosis, age and antipsychotic medication. Schizophr. Res. 98 (1–3), 16–28.

Nesvåg, R., Schaer, M., Haukvik, U.K., Westlye, L.T., Rimol, L.M., Lange, E.H., Hartberg, C.B., Ottet, M.-C., Melle, I., Andreassen, O.A., Jönsson, E.G., Agartz, I., Eliez, S., 2014. Reduced brain cortical folding in schizophrenia revealed in two independent samples. Schizophr. Res. 152 (2–3), 333–338.

Palaniyappan, L., Liddle, P., 2012. Aberrant cortical gyrification in schizophrenia: a surface-based morphometry study. J. Psychiatry Neurosci. 37, 399–406.

Palaniyappan, L., Mallikarjun, P., Joseph, V., White, T.P., Liddle, P.F., 2011. Folding of the prefrontal cortex in schizophrenia: regional differences in gyrification. Biol. Psychiatr. 69 (10), 974–979.

Palaniyappan, L., Crow, T.J., Hough, M., Voets, N.L., Liddle, P.F., James, S., Winmill, L., James, A.C., 2013. Gyrification of Broca's region is anomalously lateralized at onset of schizophrenia in adolescence and regresses at 2 year follow-up. Schizophr. Res. 147 (1), 39–45.

Pettersson-Yeo, W., Allen, P., Benetti, S., McGuire, P., Mechelli, A., 2011. Dysconnectivity in schizophrenia: where are we now? Neurosci. Biobehav. Rev. 35 (5), 1110–1124.

Rapoport, J.L., Giedd, J.N., Gogtay, N., 2012. Neurodevelopmental model of schizophrenia: update 2012. Mol. Psychiatr. 17 (12), 1228–1238.
Ronan, L., Voets, N.L., Hough, M., Mackay, C., Roberts, N., Suckling, J., Bullmore, E., James, A., Fletcher, P.C., 2012. Consistency and interpretation of changes in millimeter-scale cortical intrinsic curvature across three independent datasets in schizophrenia. Neuroimage 63 (1), 611–621.
Sasabayashi, D., Takayanagi, Y., Nishiyama, S., Takahashi, T., Furuichi, A., Kido, M., Nishikawa, Y., Nakamura, M., Noguchi, K., Suzuki, M., 2016. Increased frontal gyrification negatively correlates with executive function in patients with first-episode schizophrenia. Cerebr. Cortex bhw101.
Sasabayashi, D., Takayanagi, Y., Takahashi, T., Nemoto, K., Furuichi, A., Kido, M., Nishikawa, Y., Nakamura, M., Noguchi, K., Suzuki, M., 2019. Increased brain gyrification in the schizophrenia spectrum. Psychiatr. Clin. Neurosci. pcn.12939.
Schaer, M., Cuadra, M.B., Tamarit, L., Lazeyras, F., Eliez, S., Thiran, J.-P., 2008. A surface-based approach to quantify local cortical gyrification. IEEE Trans. Med. Imag. 27 (2), 161–170.
Schaer, M., Cuadra, M.B., Schmansky, N., Fischl, B., Thiran, J.-P., Eliez, S., 2012. How to measure cortical folding from MR images: a step-by-step tutorial to compute local gyrification index. JoVE 59, 3417.
Schmitt, J.E., Vandekar, S., Yi, J., Calkins, M.E., Ruparel, K., Roalf, D.R., Whinna, D., Souders, M.C., Satterthwaite, T.D., Prabhakaran, K., McDonald-McGinn, D.M., Zackai, E.H., Gur, R.C., Emanuel, B.S., Gur, R.E., 2015. Aberrant cortical morphometry in the 22q11.2 deletion syndrome. Biol. Psychiatr. 78 (2), 135–143.
Schultz, C.C., Koch, K., Wagner, G., Roebel, M., Nenadic, I., Gaser, C., Schachtzabel, C., Reichenbach, J.R., Sauer, H., Schlösser, R.G.M., 2010. Increased parahippocampal and lingual gyrification in first-episode schizophrenia. Schizophr. Res. 123 (2–3), 137–144.
Schultz, C.C., Koch, K., Wagner, G., Nenadic, I., Schachtzabel, C., Güllmar, D., Reichenbach, J.R., Sauer, H., Schlösser, R.G.M., 2012. Reduced anterior cingulate cognitive activation is associated with prefrontal–temporal cortical thinning in schizophrenia. Biol. Psychiatr. 71 (2), 146–153.
Schultz, C.C., Wagner, G., Koch, K., Gaser, C., Roebel, M., Schachtzabel, C., Nenadic, I., Reichenbach, J.R., Sauer, H., Schlösser, R.G.M., 2013. The visual cortex in schizophrenia: alterations of gyrification rather than cortical thickness—a combined cortical shape analysis. Brain Struct. Funct. 218 (1), 51–58.
Spalthoff, R., Gaser, C., Nenadić, I., 2018. Altered gyrification in schizophrenia and its relation to other morphometric markers. Schizophr. Res. 202, 195–202.
Stanfield, A.C., Moorhead, T.W.J., Harris, J.M., Owens, D.G.C., Lawrie, S.M., Johnstone, E.C., 2008. Increased right prefrontal cortical folding in adolescents at risk of schizophrenia for cognitive reasons. Biol. Psychiatr. 63 (1), 80–85.
Storvestre, G.B., Valnes, L.M., Jensen, A., Nerland, S., Tesli, N., Hymer, K.-E., Rosaeg, C., Server, A., Ringen, P.A., Jacobsen, M., Andreassen, O.A., Agartz, I., Melle, I., Haukvik, U.K., 2019. A preliminary study of cortical morphology in schizophrenia patients with a history of violence. Psychiatr. Res. Neuroimaging 288, 29–36.
Sugiyama, M., Hachiya, H., Towell, C., Vijayakumar, S., 2008. Geodesic Gaussian kernels for value function approximation. Aut. Robots 25 (3), 287–304.
Takayanagi, Y., Sasabayashi, D., Takahashi, T., Komori, Y., Furuichi, A., Kido, M., Nishikawa, Y., Nakamura, M., Noguchi, K., Suzuki, M., 2019. Altered brain gyrification in deficit and non-deficit schizophrenia. Psychol. Med. 49 (4), 573–580.
Tange, O., 2011. GNU parallel: the command-line power tool. ; login: The USENIX Magazine, 36, 42–47.
Vandergaag, M., Hoffman, T., Remijsen, M., Hijman, R., Dehaan, L., Vanmeijel, B., Vanharten, P., Valmaggia, L., Dehert, M., Cuijpers, A., 2006. The five-factor model of the Positive and Negative Syndrome Scale II: a ten-fold cross-validation of a revised model. Schizophr. Res. 85 (1–3), 280–287.
Veronese, E., Castellani, U., Peruzzo, D., Bellani, M., Brambilla, P., 2013. Machine learning approaches: from theory to application in schizophrenia. Comput. Math. Methods Med. 2013, 867924.
Vogeley, K., Schneider-Axmann, T., Pfeiffer, U., Tepest, R., Bayer, T.A., Bogerts, B., Honer, W.G., Falkai, P., 2000. Disturbed gyrification of the prefrontal region in male schizophrenic patients: a morphometric postmortem study. Am. J. Psychiatr. 157 (1), 34–39.
Wheeler, D.G., Harper, C.G., 2007. Localised reductions in gyrification in the posterior cingulate: schizophrenia and controls. Prog. Neuro Psychopharmacol. Biol. Psychiatr. 31 (2), 319–327.
Wheeler, A.L., Voineskos, A.N., 2014. A review of structural neuroimaging in schizophrenia: from connectivity to connectomics. Front. Hum. Neurosci. 8.
White, T., Hilgetag, C.C., 2011. Gyrification and neural connectivity in schizophrenia. Dev. Psychopathol. 23 (1), 339–352.
Woods, S.W., 2003. Chlorpromazine equivalent doses for the newer atypical antipsychotics. J. Clin. Psychiatr. 64, 663–667.
World Medical Association, 2013. World medical association declaration of Helsinki: ethical principles for medical research involving human subjects. J. Am. Med. Assoc. 310, 2191–2194.
Yan, J., Cui, Y., Li, Q., Tian, L., Liu, B., Jiang, T., Zhang, D., Yan, H., 2019. Cortical thinning and flattening in schizophrenia and their unaffected parents. Neuropsychiatric Dis. Treat. 15, 935–946.
Yuan, K., Cheng, X., Gui, Z., Li, F., Wu, H., 2019. A quad-tree-based fast and adaptive Kernel Density Estimation algorithm for heat-map generation. Int. J. Geogr. Inf. Sci. 33 (12), 2455–2476.
Zilles, K., Armstrong, E., Schleicher, A., Kretschmann, H.-J., 1988. The human pattern of gyrification in the cerebral cortex. Anat. Embryol. 179 (2), 173–179.
Zuliani, R., Delvecchio, G., Bonivento, C., Cattarinussi, G., Perlini, C., Bellani, M., Marinelli, V., Rossetti, M.G., Lasalvia, A., McIntosh, A., Lawrie, S.M., Balestrieri, M., Ruggeri, M., Brambilla, P., 2018. Increased gyrification in schizophrenia and non affective first episode of psychosis. Schizophr. Res. 193, 269–275.